



Article

Bathyptilones: Terpenoids from an Antarctic Sea Pen, *Anthoptilum grandiflorum* (Verrill, 1879)

Santana A.L. Thomas ¹, Anthony Sanchez ², Younghoon Kee ², Nerida G. Wilson ³  and Bill J. Baker ^{1,*} 

¹ Department of Chemistry, University of South Florida, Tampa, FL 33620, USA

² Department of Cellular, Microbiology and Molecular Biology, University of South Florida, Tampa, FL 33620, USA

³ Western Australia Museum and the University of Western Australia, Perth, WA 6106, Australia

* Correspondence: bjbaker@usf.edu; Tel.: +1-(813)-974-1967; Fax: +1-(813)-974-2876

Received: 31 July 2019; Accepted: 27 August 2019; Published: 1 September 2019



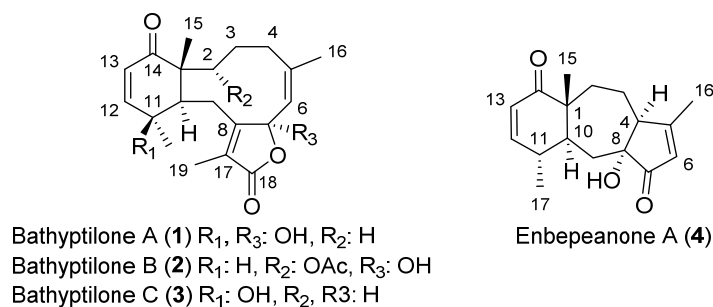
Abstract: An Antarctic coral belonging to the order Pennatulacea, collected during the 2013 austral autumn by trawl from 662 to 944 m depth, has yielded three new briarane diterpenes, bathyptilone A-C (1–3) along with a trinorditerpene, enbepeanone A (4), which bears a new carbon skeleton. Structure elucidation was facilitated by one- and two-dimensional NMR spectroscopy, mass spectrometry and confirmed by X-ray crystallography. The three compounds were screened in four cancer cell lines. Bathyptilone A displayed selective nanomolar cytotoxicity against the neurogenic mammalian cell line Ntera-2.

Keywords: briarane diterpene; cytotoxicity screening; deep sea; pennatulacea; marine natural products

1. Introduction

Since the late 1950s, marine organisms have been increasingly important as sources of novel secondary metabolites, many of which demonstrate significant biological activity. Chemical studies were enabled by technological advancements such as the development of SCUBA diving equipment in the 1950s and 1960s, and of ROVs toward the latter part of the century, providing access to increasingly diverse biological materials. However, marine organisms found in cold-water environments are still largely understudied as sources of new chemodiversity [1]. More than 90% of the ocean exists at temperatures below 3 °C, yet only 2% of natural products are reported from marine organisms collected in these regions [1,2], reflecting, in part, that such environments remain difficult to access. Despite the lack of attention, important biologically active compounds continue to be found [3–9].

Species from the order Pennatulacea are known for the production of briarane, cembrane and similar diterpenes [10]. Briarane diterpenes were first described four decades ago and the ensuing years have seen more than 600 reported in the literature [11]. They exhibited a wide range of biological activities, including cytotoxicity, anti-inflammatory, antiviral, insecticidal and immunomodulatory activity [12–16]. A benthic collection of the Pennatulacean genus *Anthoptilum* from Western Australia produced five neuroactive briaranes, the anthoptilides [17]. Herein, we describe the isolation and structure elucidation of two classes of compounds isolated from an Antarctic specimen of *Anthoptilum grandiflorum*, including (Scheme 1) briaranes, bathyptilone A–C (1–3) and the new scaffold of a trinorditerpene, enbepeanone A (4), likely derived from a briarane precursor.



Scheme 1. Structure and numbering system for bathyptilones A-C and enbepeanone A.

2. Results and Discussion

The coral *Anthoptilum grandiflorum* was collected by trawl at a depth of between 662 and 944 m during an austral autumn cruise aboard the R/V Nathaniel B. Palmer (NBP) in the vicinity of the Scotia Arc. The sea pens were frozen and freeze-dried, followed by an exhaustive extraction in refluxing DCM using a Soxhlet extractor. Normal-phase MPLC of the 10.6 g Soxhlet extract was conducted for initial fractionation. Normal- and reverse-phase HPLC yielded four new terpenoid metabolites (1–4).

Bathyptilone A (1) was isolated as a crystalline solid with a molecular formula of $C_{20}H_{26}O_5$, based on HRESIMS with supporting 1H and ^{13}C NMR data (Table 1). The ^{13}C NMR spectrum indicated the presence of a ketone, an ester-equivalent, four quaternary, four methine, four methylene and four methyl groups, accounting for all carbons and twenty-four of the twenty-six protons. Further, one quaternary carbon had a shift (δ_C 69.3) indicative of an oxygen-bearing sp^3 carbon, while a second quaternary carbon (δ_C 106.2) appeared as a ketal-type carbon. A tricyclic scaffold was derived by the degree of unsaturation, as five of the eight unsaturations could be assigned to double bond functions (ketone, δ_C 203.7; ester-equivalent, δ_C 171.7; and six olefinic carbons, δ_C 160.7, 151.7, 145.3, 127.4, 125.8, 124.1).

Table 1. NMR Spectroscopic Data for Bathyptilone A (1).

Position	^{13}C , type	1H (J in Hz)	HMBC
1	50.2, C		
2	21.8, CH_2	a 1.54, m b 1.84, m	14 1, 4
3	31.6, CH_2	a 1.52, m b 1.98, m	2 1, 2, 4, 10, 15
4	29.5, CH_2	a 1.85, m b 3.52, br t	5, 6
5	145.3, C		
6	124.1, CH	5.35, s	4, 5, 7, 16
7	106.2, C		
8	160.7, C		
9	22.7, CH_2	a 2.47, d (15.8) b 3.25, dd (9.5, 15.3)	1, 8, 10, 11, 17 7, 8, 10, 11, 17
10	41.4, CH	3.14, d (9.5)	1, 8, 9, 11, 14, 15
11	69.3, C		
12	151.7, CH	6.63, d (10.0)	10, 11, 14, 20
13	127.4, CH	5.97, d (10.0)	1, 11
14	203.7, C		
15	24.2, CH_3	1.16, s	1, 2, 3, 10, 14
16	23.5, CH_3	1.78, s	4, 5, 6
17	125.8, C		
18	171.7, C		
19	9.1, CH_3	1.95, s	8, 17, 18
20	30.4, CH_3	1.35, s	10, 11, 12
	7, 11-OH	3.52, br	

A cyclohexenone ring was constructed from COSY and HMBC data. Two $^3J_{\text{HH}}$ coupled olefinic protons (Figure 1), δ_{H} 6.63 (H-12) and δ_{H} 5.97 (H-13), displayed HMBC correlations to δ_{C} 203.7 (C-14), establishing an α,β -unsaturated ketone. Proton H-12 displayed further HMBC connectivity to an aliphatic methine δ_{C} 41.4 (C-10), as well as to a quaternary, oxygen-bearing carbon (δ_{C} 69.3, C-11). Proton H-13 similarly extended the cyclohexenone substructure with HMBC correlation to an aliphatic quaternary carbon (δ_{C} 50.2, C-1), which, by virtue of correlations from a methyl singlet that networked C-1, -10, -14, into the HMBC spin system, completed the cyclohexenone substructure (Figure 1). The cyclohexenone portion could be decorated at C-11 with the C-20 methyl group (δ_{C} 30.4), which displayed HMBC correlations to C-10, -11 and -12 (δ_{C} 151.7). Additional corroboration of the six-membered ring was obtained from H-10, with HMBC correlations to C-1 and C-11. This cyclohexenone partial structure has two open valences, at C-1 and C-10.

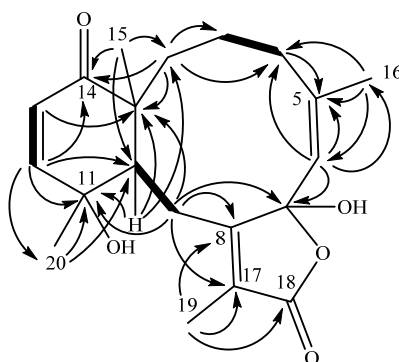


Figure 1. Key COSY (—) and HMBC (→) correlations establishing the planar structure of bathyptilone A (**1**).

The elaboration of the cyclohexenone resulted in a fused cyclodecene ring. Besides previously described correlations into the cyclohexenone ring, H₃-15 (δ_{H} 1.16) displayed a further correlation to a methylene carbon at δ_{C} 21.8 (C-2). Although proton H-2a (δ_{H} 1.54) and H-2b (δ_{H} 1.84) overlapped protons of H-3a (δ_{H} 1.52) and H-4a (δ_{H} 1.85), respectively, preventing clear assignment of COSY correlations, it was observed that H-2b and C-4 (δ_{C} 29.5) were correlated in the HMBC spectrum. Both H-3a and H-3b displayed HMBC correlations to C-2, and H-3b further correlated to C-1 (δ_{C} 50.2), establishing an alkyl substituent at C-1. Proton H-4a was found to extend the alkyl group through HMBC correlations to two olefinic carbons, C-5 (δ_{C} 145.3) and C-6 (δ_{C} 124.1). The HMBC also established that quaternary C-5 bears a vinyl methyl δ_{H} 1.78 (H₃-16) based on HMBC correlations of H-6 (δ_{C} 5.35) to C-16 (δ_{C} 23.5) and reciprocal correlations from H₃-16 to C-6, as well as C-5 (δ_{C} 145.3). Further development of this partial structure ended at a quaternary, acetal-type carbon at δ_{C} 106.2 (C-7) based on an HMBC correlation from H-6.

An isolated spin system was observed in the COSY spectrum between the broad doublet δ_{H} 3.14 (H-10) and the doublet of doublets δ_{H} 3.25 (H-9b), the latter of which also correlated to H-9a (δ_{H} 2.47). HMBC extended that system further based on H₂-9 correlations to two quaternary olefinic carbons, C-8 (δ_{C} 160.7) and C-17 (δ_{C} 125.8). A key correlation between H-9a and the acetal-like carbon C-7 (δ_{C} 106.2) completed a C₁₀ macrocycle.

Remaining to be accounted were an ester-type carbon (δ_{C} 171.7, C-18) and a vinyl methyl group (δ_{H} 1.95, H₃-19), and two open valencies on C-7 (δ_{C} 106.2) and C-17 (δ_{C} 125.8). The vinyl methyl group correlated in the HMBC spectrum to quaternary olefins C-8 and C-17, locating the methyl group on one of the open valencies on C-17. Methyl protons H₃-19 also displayed an HMBC correlation to C-18, accounting for all the carbon atoms in the molecular formula and requiring that the remaining two oxygen atoms occupy the open valencies on C-7 and C-18, resulting in a γ -lactone bearing a C-7 hemiacetal. The planar structure that results from these connections identifies bathyptilone A (**1**) as a member of the briarane family of octocoral metabolites.

The stereochemical evaluation of bathyptilone A (**1**) was approached using NOESY spectroscopy. Proton H-10 (δ_{H} 3.14) showed NOESY correlations to δ_{H} 1.35 (H₃-20) and δ_{H} 3.52 (H-4b), while H₂-9 (δ_{H} 2.47, H-9a; 3.25, H-9b) displayed proximity to H₃-15 (δ_{H} 1.16), setting the ring fusion *trans*, as observed in all other briarane diterpenes [11], with H₃-20 occupying the same face of the ring fusion as H-10. The remaining stereogenic carbon, C-7, lacked a proton, but correlation between the 7-OH/11-OH overlapping hydroxyl signal in the ¹H NMR spectrum, δ_{H} 3.52, and H-10 must result from 7-OH rather than 11-OH, which has already been shown to be on the opposite face of the tricycle from H-10. These stereocenters, as well as the configuration of the C-7 hemiacetal, were confirmed by X-ray crystallography analysis (Figure 2, Table S1), which facilitated the assignment of the absolute configuration of bathyptilone A as depicted in **1**.

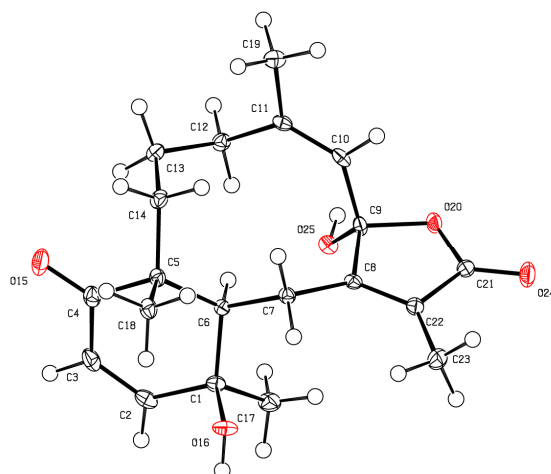


Figure 2. Asymmetric unit of bathyptilone A (**1**). Anisotropic displacement parameters were drawn at 50% probability.

The molecular formula of bathyptilone B (**2**) was established as C₂₂H₂₈O₆ by HRESIMS and supported by ¹H and ¹³C NMR data (Table 2), which appears to differ by the acetylation of bathyptilone A (**1**). This was confirmed by observation of ¹³C NMR signals for the two additional carbons as an ester-type carbonyl at δ_{C} 169.5 (C-21) and an aliphatic methyl at δ_{C} 21.2 (C-22), the latter bearing protons that were found in the ¹H NMR spectrum as a 3H singlet at δ_{H} 2.03 (H₃-22). This substituent could be placed at C-2 (δ_{C} 77.9) based on a deshielded proton at δ_{H} 5.89 (H-2), which correlated in the HMBC spectrum to carbons that matched their bathyptilone A analog, including δ_{C} 52.5 (C-1) and δ_{C} 41.4 (C-10), as well as the new carbon at C-21 (Figure 3). With new oxidation at C-2, relative to bathyptilone A, C-11 (δ_{C} 38.0) was compared between **1** and **2** and found to be proton bearing rather than oxygen bearing.

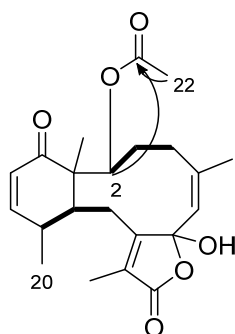


Figure 3. Key COSY (—) and HMBC (→) correlations establishing the differences between bathyptilone A (**1**) and B (**2**).

Table 2. ^1H and ^{13}C NMR Data for Bathyptilone B (2) and Bathyptilone C (3).

Position	Bathyptilone B (2)		Bathyptilone C (3)	
	C, type ^{a,c}	^1H (J in Hz) ^b	C, type	^1H (J in Hz)
1	52.5, C		50.5, C	
2	77.9, CH	5.89, dd (4.8, 12.9)	31.5, CH ₂	a 1.90, m b 1.56, m
3	27.6, CH ₂	a 3.93, dt (3.2, 14.7) b 1.89, m	21.8, CH ₂	a 1.95, m b 1.52, m
4	26.3, CH ₂	a 1.99, m b 2.32, m	30.3, CH ₂	a 2.60, td (13.5, 5.3) b 2.03, m
5	146.0, C		141.2, C	
6	122.8, CH	5.26, s	122.4, CH	5.00, br d (8.6)
7	106.3, C		79.2, CH	5.66, br d (8.2)
8	161.3, C		159.4, C	
9	28.4, CH ₂	a 3.64, m b 2.40, m	22.4, CH ₂	a 3.28, br dd (15.6, 9.7) b 2.34, br d (15.6)
10	41.4, CH	3.34, t (8.5)	44.8, CH	2.42, br d (9.3)
11	38.0, CH	2.45, m	68.9, C	
12	154.8, CH	6.64, br d (10.3)	151.2, CH	6.62, br d (9.7)
13	127.0, CH	5.94, d (10.3)	127.6, CH	6.00, br d (9.7)
14	201.4, C		203.2, C	
15	16.7, CH ₃	1.11, s	24.0, CH ₃	1.14, s
16	23.2, CH ₃	1.77, s	22.7, CH ₃	1.74, s
17	124.3, C		122.9, C	
18	171.7, C	1.91, s	163.9, C	
19	9.1, CH ₃		9.1, CH ₃	1.94, s
20	18.8, CH ₃	1.14, d (6.5)	30.8, CH ₃	1.27, s
21	169.5, C			
22	21.2, CH ₃	2.03, s		

As for bathyptilone A (1), bathyptilone B (2) was evaluated by 2D-NOE to determine the configuration of the asymmetric centers. H₃-15 (δ_{H} 1.11) correlates to both H-2 (δ_{H} 5.89) and H-11 (δ_{H} 2.45), placing them on the same face of the bicyclic ring system, while H-10 (δ_{H} 3.43) only correlated to H-3a (δ_{H} 3.93). This evaluation supported the usual observation of the *trans* configured C-1/10 bridge in briarane-type scaffolds. X-ray crystallography (Figure 4) corroborated these assignments.

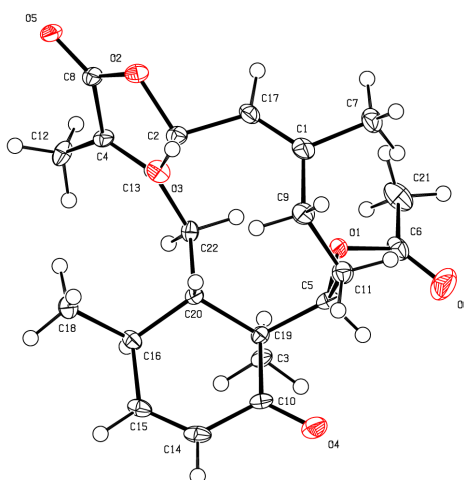


Figure 4. Asymmetric unit of bathyptilone B (2). Anisotropic displacement parameters were drawn at 50% probability.

Analysis of the crystalline bathyptilone C (3) with HRESIMS and 1D ^1H and ^{13}C NMR spectra yielded a molecular formula of C₂₀H₂₆O₄. The ^1H NMR spectrum of 3 showed shifts similar to

compound **1** with the addition of a methine at δ_{H} 5.66 (H-7). The ^{13}C NMR spectrum was closely matched to that of bathyptilone A, with the major difference being the upfield shift of C-7 (δ_{C} 79.2), which indicated the replacement of the bathyptilone A hemiacetal functionality by an alcohol function. Stereochemical analysis using NOE correlations, as well as comparison of shifts to bathyptilone A (**1**), established bathyptilone C as the C-7 reduced analog of **1**, an assignment which was confirmed by X-ray analysis (Figure 5).

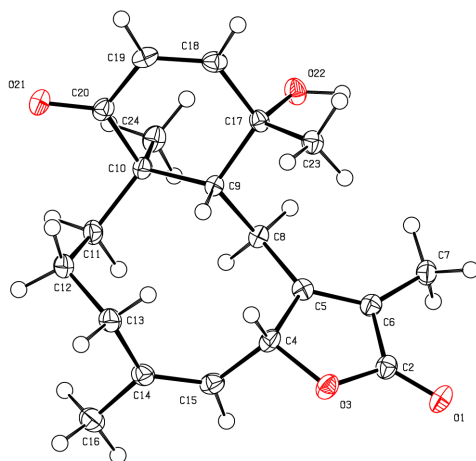


Figure 5. Asymmetric unit of bathyptilone C (**3**). Anisotropic displacement parameters were drawn at 50% probability.

A fourth compound (**4**) isolated from *Anthoptilum grandiflorum* was determined to have the molecular formula $\text{C}_{17}\text{H}_{22}\text{O}_3$ based on HRESIMS. 1D ^1H and ^{13}C NMR spectra (Table 3) suggested that compound **4** was a terpenoid, despite the odd carbon count. There were seven degrees of unsaturation that were accounted for by the presence of two ketone carbonyls, two olefins and a tricyclic ring system. Initially, COSY was used to identify two isolated spin systems. Starting with the most deshielded protons, δ_{H} 6.57 (H-12) and δ_{H} 6.07 (H-13) were coupled and H-12 further coupled to aliphatic methine δ_{H} 2.08 (H-11). The spin system bifurcated at H-11, with the system terminating in one direction with a methyl group at δ_{H} 1.09 (H₃-17) but extending the system in the other direction to a methylene at δ_{H} 1.35 (H-10). The second spin system established by COSY was found as a methine at δ_{H} 2.20 (H-4) coupled to δ_{H} 1.20 (H-3a). Proton H-4 was extended by HMBC to an α,β -unsaturated ketone based on correlation to δ_{C} 177.5 (C-5), δ_{C} 133.2 (C-6), δ_{C} 205.4 (C-7), and δ_{C} 99.5 (C-8). Proton H-4 further correlated in the HMBC spectrum to a vinyl methyl at δ_{H} 2.09 (H₃-16). The remaining methyl group, δ_{C} 19.3 (C-15), was assigned based on HMBC correlations to δ_{C} 52.8 (C-1), δ_{C} 31.9 (C-2) and δ_{C} 202.9 (C-14). The complete two-dimensional structure of **4** was completed by connecting the first COSY spin system to C-1, C-8 and C-14, as depicted in Figure 6.

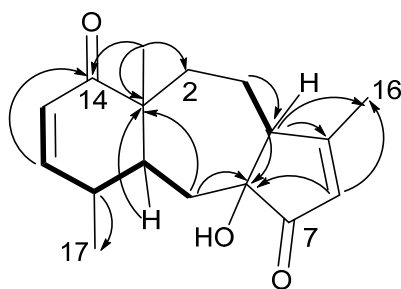


Figure 6. Key COSY (—) and HMBC (→) correlations of enbepeanone A (**4**).

Table 3. NMR data for enbepeanone A (4).

Position	^{13}C , type	^1H (J in Hz)
1	52.8, C	1.14, m
2	31.9, CH ₂	1.39, m
3	19.5, CH ₂	1.20, m
4	46.3, CH	1.30, m
5	177.5, C	2.20, m
6	133.2, CH	5.85, s
7	205.4, C	
8	99.5, C	
9	28.3, CH ₂	1.36, m
10	32.2, CH	1.46, dd (12.4, 7.0)
11	36.1, CH	1.35, m
12	153.6, CH	2.08, m
13	128.0, CH	6.57, dd (10.9, 6.2)
14	202.9, C	6.07, d (10.9)
15	19.3, CH ₃	1.24, s
16	25.7, CH ₃	2.09, s
17	19.6, CH ₃	1.09, d (6.8)

The stereochemistry of enbepeanone A (**4**) was assigned from NOESY. Proton H-10 showed a strong correlation to the methyl doublet, which indicated their proximity; however, the methyl singlet of H-15 did not have a NOESY correlation to H-10 as noted for the briarane scaffolds in the bathyptilones. The cyclopentenone stereocenters, and their relationship to the cyclohexenone, were established by X-ray crystallographic analysis (Figure 7). The crystallographic metadata (Table S4) facilitated the assignment of the absolute configuration of enbepeanone A as shown.

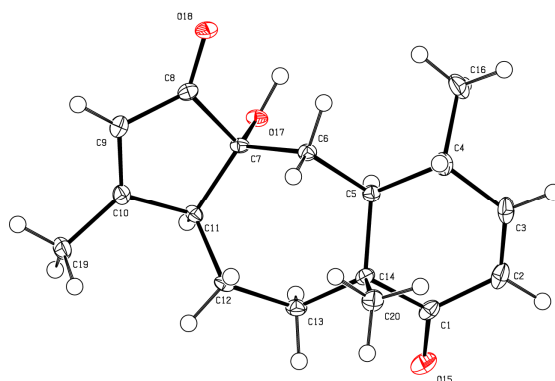
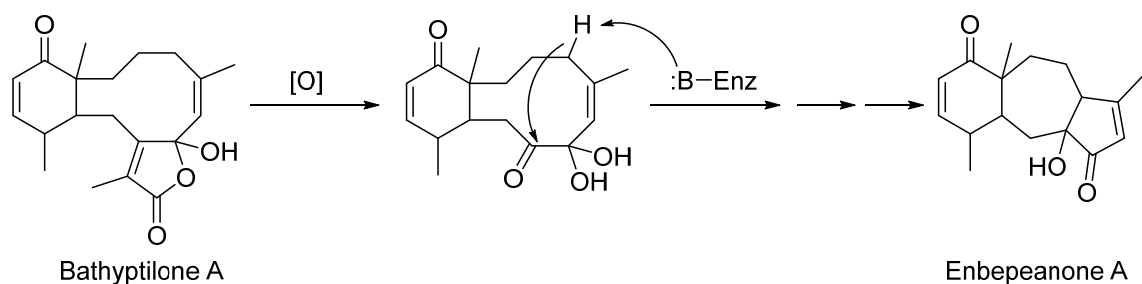


Figure 7. Asymmetric unit of enbepeanone A (**4**). Anisotropic displacement parameters were drawn at 50% probability.

Enbepeanone A (**4**) is a trinorditerpene seemingly derived from the oxidation of a briarane skeleton such as bathyptilone A (**1**). Oxidative cleavage of the C-8 pendant isopropyl group from **1** provides an intermediate suited to enzyme-catalyzed cyclopentanulation that would produce the enbepeanone A skeleton (Scheme 2). This is the first example of such a trinorditerpene bearing this carbon skeleton.



Scheme 2. Hypothetical biochemical conversion of briarane bathyptilone A (1) into the enbepeanone skeleton.

Several mammalian cell types were analyzed for sensitivity to these diterpenes (Figure 8). Of the compounds tested, bathyptilone A (1) was highly toxic to a pluripotent embryonal carcinoma cell line, NTera-2 (NT2). This cell line was isolated from a lung metastasis of testicular cancer; however, these cells exhibit many properties of precursor neuronal cells like the formation of neurons and the presence of homeobox clusters in the genome [18]. Due to their similarity with developing neuronal cells, this cell line is accepted as a valid system for the assessment of neurotoxicity [19]. Compound 1 effectively killed the NT2 cells at with an IC_{50} of 29 nM. A recent publication describes the promising antiproliferative effect of gedunin with an IC_{50} as low as 13.5 μ M against NT2 cells [20]. Compounds 2–4 were also tested against the NT2 cell line, but their activities were not significant. Based on this finding, we speculate that bathyptilone A may prove to be an effective therapeutic strategy for specifically targeting neuronal cancers.

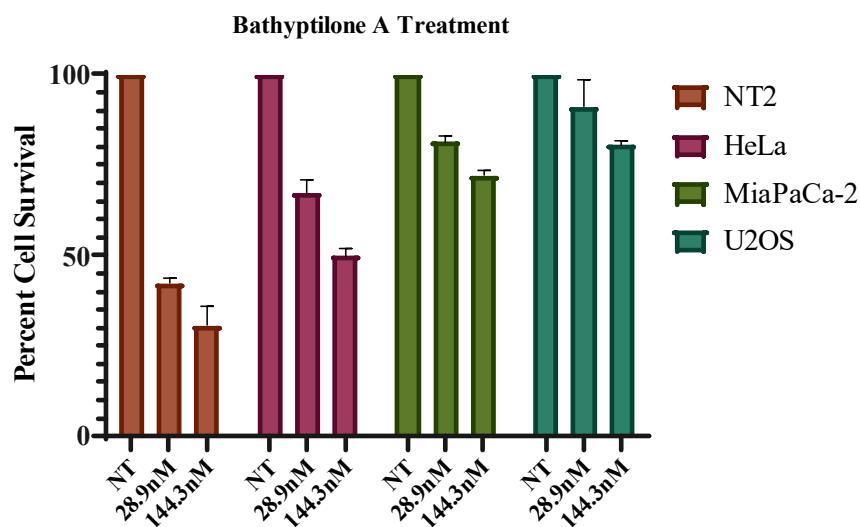


Figure 8. Bioactivity of bathyptilone A (1) against NT2, HeLa, MiaPaca-2 and U2OS cell lines. NT, no treatment.

3. Experimental Section

3.1. General Experimental Procedure

Optical Rotations were measured by a Rudolph Instruments (Hackettstown, NJ, USA) AutoPol IV polarimeter at 589 nm. UV absorptions were measured by an Agilent (Santa Clara, CA, USA) Cary 60 UV-Vis spectrophotometer; wavelengths are recorded in nm. IR spectra were recorded with a PerkinElmer (Waltham, MA, USA) Spectrum Two with a UATR (single-reflection diamond) sample introduction system; peaks are reported in cm^{-1} . NMR spectra were recorded at 298 K on an Agilent (Santa Clara, CA, USA) Varian Direct Drive 500 or Varian Direct Drive 800 MHz NMR spectrometers. Chemical shifts are reported with the use of the residual $CDCl_3$ signals (δ_H 7.27 ppm; δ_C 77.0 ppm) as

internal standards for ^1H and ^{13}C NMR spectra. The ^1H and ^{13}C NMR assignments were supported by COSY, HSQC, HMBC, and NOESY experiments. The high-resolution mass spectra were recorded on an Agilent (Santa Clara, CA, USA) 6230 TOF LC/MS. Semi-preparative and analytical HPLC was performed on a Shimadzu (Columbia, MD, USA) LC-20 AT system equipped with an evaporative light-scattering detector (ELSD) and a ultraviolet detector using a Luna column (5 μm , 250 \times 10 mm) and a YMC (Kyoto, Japan) packed column (10 μm , 150 \times 4 mm). MPLC was performed on a Teledyne Isco (Lincoln NE) CombiFlash Rf 200i equipped with an ELSD using a RediSep Rf silica 120 g flash column with silica gel 230–400 mesh ASTM used to load the sample.

3.2. Animal Material

Specimens of the pennatulacean octocoral *Anthoptilum grandiflorum* were collected in April 2013, north of Burdwood Bank (54°14'56.9" S, 59°00'00.6" W), by trawling on the R/V Nathaniel B. Palmer from depths of between 662 and 944 meters. A specimen voucher is retained at the Scripps Institution of Oceanography Benthic Invertebrate collection (SIO-BIC Co2892, field number S22350). A piece of tissue from this voucher was extracted with a DNeasy kit (Qiagen) and was amplified for the mitochondrial msh1 (muts homolog) to confirm identification. We used the primers ND42599F/mut3458R [21,22] to produce amplicons and outsourced these for sequencing (AGRF Perth node). The resulting bi-directional sequence was compared to other available Pennatulacea sequences in GenBank using a Maximum-Likelihood analysis at the W-IQ-tree server [23]. W-IQ-Tree incorporates the ModelTest [24], which selected the K3P + G4 as the best-fit model, and which is automatically applied. The tree topology was assessed using 1000 ultrafast bootstrap replicates and shows that our specimen has an identical msh1 sequence to a specimen of *Anthoptilum grandiflorum* from Greenland (Supplementary information) [25]. The species has been recorded as having a worldwide distribution [26], although this study represents the southernmost record of this species.

3.3. Isolation of Bathyptilones and Enbepeanone

The *Anthoptilum grandiflorum* was immediately frozen after collection and later freeze-dried at our lab. The lyophilized organism (84.7 g) was then broken into smaller pieces and exhaustively extracted via 3 cycles of DCM (3.5 L) in a Soxhlet extractor. The crude extract (11.7 g) was partitioned through liquid–liquid extraction using DCM and water. The organic layer (10.4 g) was then concentrated, resulting in a brownish residue, and then re-suspended in DCM to be dried onto silica gel for flash chromatography using MPLC. A concentration gradient of hexane and ethyl acetate was extended over a period of time to elute 8 fractions (A–H). Fraction E (191.0 mg) eluted in 9:11 hexane/ethyl acetate and was subjected to further purification in normal phase HPLC on a silica gel column to afford 11 fractions. Fractions 4, 6, and 9 afforded the tricyclic diterpene compounds, bathyptilone A (**1**, 3.6 mg), B (**2**, 2.1 mg), C (**3**, 1.8 mg) and enbepeanone A (**4**, 0.7 mg) with further purification on a C_{18} reverse-phase HPLC column. The crystallization of these compounds occurred through slow evaporation using the mobile-phase solvents.

Bathyptilone A (1): Crystalline solid; $[\alpha]_{\text{D}}^{24} -18.3$ (c 0.11, CHCl_3); UV λ_{max} (EtOH) (log ϵ) 271 nm; IR 3650, 3356, 2980, 2646, 2322, 2286, 2166, 1738, 1656, 1446, 1378, 1212, 1114, 934, 892, 834, 754 cm^{-1} ; ^1H NMR (500 MHz, CDCl_3) and ^{13}C NMR (125 MHz, CDCl_3), see Table 1; HRESIMS m/z 347.1853 $[\text{M} + \text{H}]^+$ (347.1859 calculated for $\text{C}_{20}\text{H}_{27}\text{O}_5$).

Bathyptilone B (2): Crystalline solid; $[\alpha]_{\text{D}}^{24} -40.2$ (c 0.11, CHCl_3); IR 3346, 2980, 2886, 1736, 1662, 1456, 1378, 1230, 938, 752 cm^{-1} ; ^1H NMR (800 MHz, CDCl_3), see Table 2 and ^{13}C NMR (200 MHz, CDCl_3), see Table 2; HRESIMS m/z 411.1775 $[\text{M} + \text{Na}]^+$ (411.1784 calculated for $\text{C}_{22}\text{H}_{28}\text{O}_6\text{Na}$).

Bathhyptilone C (3): Crystalline solid; $[\alpha]_D^{24} -16.2$ (c 0.11, CHCl_3); $^1\text{H NMR}$ (800 MHz, CDCl_3), see Table 2 and $^{13}\text{C NMR}$ (200 MHz, CDCl_3), see Table 2; HRESIMS m/z 330.1842 $[\text{M} + \text{H}]^+$ (330.1831 calculated for $\text{C}_{20}\text{H}_{27}\text{O}_4$).

Enbepeanone A (4): Crystalline solid; $[\alpha]_D^{24} -11.0$ (c 0.11, CHCl_3); IR 3424, 3190, 2646, 2322, 1650, 1020, 742, 512, 456, 414 cm^{-1} ; $^1\text{H NMR}$ (500 MHz, CDCl_3) and $^{13}\text{C NMR}$ (125 MHz, CDCl_3), see Table 3; HRESIMS m/z 275.1640 $[\text{M} + \text{H}]^+$ (275.1647 calculated for $\text{C}_{17}\text{H}_{23}\text{O}_3$).

3.4. X-Ray Crystallography

The X-ray diffraction data were measured on a Bruker D8 Venture PHOTON 100 CMOS system (Madison, WI, USA) equipped with a Cu K_α INCOATEC ImuS micro-focus source ($\lambda = 1.54178 \text{ \AA}$). Indexing was performed using Apex3 [27]. Data integration and reduction were performed using SaintPlus 6.01 [28]. Absorption correction was performed by a multi-scan method implemented in SADABS [29]. Space groups were determined using XPREP implemented in APEX3 [27]. Structures were solved using SHELXT [30] and refined using SHELXL-2017 [31–33] (full-matrix least-squares on F^2) through the OLEX2 interface program [34]. All non-hydrogen atoms were refined anisotropically. The hydrogen atoms of $-\text{OH}$ groups were freely refined. The remaining hydrogen atoms were placed in geometrically calculated positions and were included in the refinement process using a riding model with isotropic thermal parameters. Crystal data and refinement conditions are shown in Supplementary Tables S1–S5. The absolute configuration for compounds 1 and 3 was established based on the Flack parameter value and verified additionally with Bijvoet–Pair Analysis and Bayesian Statistics Methods [35,36] (Table S5). $P_2 \approx 1$ for all cases and this represents the probability that the current model is correct assuming the possibility that one out of two enantiomers is present. The results of the absolute configuration assignments for compound 2 are not conclusive.

Crystallographic data for the structures reported in this paper have been deposited with the Cambridge Crystallographic Data Centre as supplementary publication nos. CCDC 1,944,295 for 1, CCDC 1,944,292 for 2, CCDC 1,944,293 for 3 and CCDC 1,944,294 for 4. Copies of the data can be obtained, free of charge, on application to the Director, CCDC, 12 Union Road, Cambridge CB2 1EZ, UK.

Crystallographic data for bathhyptilone A (1). $\text{C}_{20}\text{H}_{26}\text{O}_5$, $M = 346.41$, crystal size $0.093 \times 0.038 \times 0.034 \text{ mm}^3$, orthorhombic, $a = 8.7926(2) \text{ \AA}$, $b = 12.2611(2) \text{ \AA}$, $c = 16.4222(3) \text{ \AA}$, $\alpha = \beta = \gamma = 90^\circ$, $V = 1770.43 (6) \text{ \AA}^3$, $T = 100.01 \text{ K}$, space group $P2_12_12_1$, $Z = 4$, $D_{\text{calcd}} = 1.300 \text{ g/cm}^3$, $\mu = 0.753 \text{ mm}^{-1}$, $F(000) = 744.0$, 3123 independent reflections ($R_{\text{int}} = 0.0453$, $R_{\text{sigma}} = 0.0213$). The final $R_1 = 0.0288$ ($I \geq 2\sigma(I)$), $wR_2 = 0.0674$ ($I \geq 2\sigma(I)$), $R_1 = 0.0312$ (all data), $wR_2 = 0.0688$ (all data), $S = 1.088$. The Flack parameter was -0.04 (6).

Crystallographic data for bathhyptilone B (2). $\text{C}_{22}\text{H}_{28}\text{O}_6$, $M = 388.44$, crystal size $0.04 \times 0.02 \times 0.005 \text{ mm}^3$, monoclinic, $a = 9.5139(4) \text{ \AA}$, $b = 10.3255(5) \text{ \AA}$, $c = 10.4615(4) \text{ \AA}$, $\alpha = \gamma = 90^\circ$, $\beta = 90.924^\circ$ (3), $V = 1027.56 (8) \text{ \AA}^3$, $T = 100.02 \text{ K}$, space group $P2_1$, $Z = 2$, $D_{\text{calcd}} = 1.255 \text{ g/cm}^3$, $\mu = 0.744 \text{ mm}^{-1}$, $F(000) = 416.0$, 3614 independent reflections ($R_{\text{int}} = 0.1118$, $R_{\text{sigma}} = 0.1052$). The final $R_1 = 0.0576$ ($I \geq 2\sigma(I)$), $wR_2 = 0.1076$ ($I \geq 2\sigma(I)$), $R_1 = 0.0859$ (all data), $wR_2 = 0.1184$ (all data), $S = 1.041$. The Flack parameter was 0.2 (3).

Crystallographic data for bathhyptilone C (3). $\text{C}_{20}\text{H}_{26}\text{O}_4$, $M = 330.41$, crystal size $0.467 \times 0.058 \times 0.055 \text{ mm}^3$, orthorhombic, $a = 8.2529(2) \text{ \AA}$, $b = 10.8806(3) \text{ \AA}$, $c = 19.0878(5) \text{ \AA}$, $\alpha = \beta = \gamma = 90^\circ$, $V = 1714.02 (8) \text{ \AA}^3$, $T = 99.99 \text{ K}$, space group $P2_12_12_1$, $Z = 4$, $D_{\text{calcd}} = 1.280 \text{ g/cm}^3$, $\mu = 0.707 \text{ mm}^{-1}$, $F(000) = 712.0$, 3597 independent reflections ($R_{\text{int}} = 0.0725$, $R_{\text{sigma}} = 0.0359$). The final $R_1 = 0.0356$ ($I \geq 2\sigma(I)$), $wR_2 = 0.0852$ ($I \geq 2\sigma(I)$), $R_1 = 0.0398$ (all data), $wR_2 = 0.0885$ (all data), $S = 1.071$. The Flack parameter was 0.03 (9).

Crystallographic data for enbepeanone A (4). $\text{C}_{17}\text{H}_{22}\text{O}_3$, $M = 274.34$, crystal size $0.2 \times 0.06 \times 0.02 \text{ mm}^3$, orthorhombic, $a = 7.1483(2) \text{ \AA}$, $b = 7.7391(2) \text{ \AA}$, $c = 25.4330(7) \text{ \AA}$, $\alpha = \beta = \gamma = 90^\circ$, $V = 1406.99 (7) \text{ \AA}^3$, $T = 100.0 \text{ K}$, space group $P2_12_12_1$, $Z = 4$, $D_{\text{calcd}} = 1.295 \text{ g/cm}^3$, $\mu = 0.698 \text{ mm}^{-1}$, $F(000) = 592.0$, 2884

independent reflections ($R_{\text{int}} = 0.0551$, $R_{\text{sigma}} = 0.0432$). The final $R_1 = 0.0374$ ($I \geq 2\sigma(I)$), $wR_2 = 0.0789$ ($I \geq 2\sigma(I)$), $R_1 = 0.0455$ (all data), $wR_2 = 0.0825$ (all data), $S = 1.105$. The Flack parameter was -0.03 (13).

3.5. Biological Assays

Ntera-2, MiaPaca-2, HeLa and U2OS cell lines. Several cell lines were tested for sensitivity to the tricyclic diterpenes, the cell lines tested were HeLa (ATCC CCL-2™), MiaPaCa-2 (ATCC CRL-1420™), U2OS (ATCC HTB-96™), and NT2 (ATCC CRL-1973™). All cells used were seeded into 96-well plates (~25 cells per well) and allowed to attach for 48 h under normal growth conditions (described below). Compounds were administered at the indicated concentrations and the cells were allowed to grow for 10 days. All cell lines used were grown in Dulbecco's Modification of Eagle's Medium (DMEM), with 4.5 g/L glucose and L-glutamine (Corning, 10-107-CV) supplemented with 10% Fetal Bovine Serum (Seradigm, 3100-500) and 1% penicillin–streptomycin–glutamine (HyClone, SV30082.01). All cell lines were grown at 37 °C with 5% CO₂ in a FORMA Series II Water Jacket CO₂ Incubator (Thermo). After the growth period, the cells were fixed with a 10% methanol + 10% acetic acid solution for 15 minutes at room temperature. The fixed cells were stained with crystal violet for 5 minutes and destained by washing with water. The cells were dried overnight. Crystal violet was removed from the cells with Sorensen buffer (0.1M sodium citrate, 50% ethanol), the colorimetric intensity of each solution was quantified using Gen5 software on a Synergy 2 (BioTek, Winooksi, VT, USA) plate reader (OD at 595 nm). Error bars are representative of 3 independent experiments.

Supplementary Materials: The following are available online at <http://www.mdpi.com/1660-3397/17/9/513/s1>.

Author Contributions: Conceptualization, N.G.W., Y.K. and B.J.B.; Methodology, S.A.L.T and A.S.; Resources, N.G.W, Y.K. and B.J.B.; Data Curation, N.G.W, Y.K. and B.J.B.; Writing—Original Draft Preparation, S.A.L.T. and B.J.B.; Writing—Review and Editing, S.A.L.T., A.S., Y.K., N.G.W. and B.J.B.; Supervision, Y.K. and B.J.B.; Funding Acquisition, N.G.W, Y.K. and B.J.B.

Funding: Funding for this project was provided by grants ANT-1043749 (N.G.W.), ANT-0838776 and PLR-1341339 (to B.J.B.), from the Antarctic Organisms and Ecosystems program of the National Science Foundation, and the ACE expedition (carried out by the Swiss Polar Institute, supported by the ACE Foundation and Ferring Pharmaceuticals).

Acknowledgments: We would like to thank the scientists and crew aboard the Nathaniel B. Palmer that aided our research efforts during the 2013 research cruise. For the crystallographic data, we thank Lukasz Wojtas and Gaurav Verma for their assistance. Greg W. Rouse, Scripps Institution of Oceanography, was instrumental in the logistical and conceptual implementation of the field work. We are grateful for screening against ESKAPE pathogens in the lab of Lindsey Shaw.

Conflicts of Interest: The authors declare no conflict of interest.

References

1. Soldatou, S.; Baker, B.J. Cold-water marine natural products, 2006 to 2016. *Nat. Prod. Rep.* **2017**, *34*, 585–626. [[CrossRef](#)]
2. Blunt, J.W.; Copp, B.R.; Keyzers, R.A.; Munro, M.H.G.; Prinsep, M.R. Marine natural products. *Nat. Prod. Rep.* **2015**, *32*, 116–211. [[CrossRef](#)]
3. Trimurtulu, G.; Faulkner, D.J.; Perry, N.B.; Ettouati, L.; Litaudon, M.; Blunt, J.W.; Munro, M.H.G.; Jameson, G.B. Alkaloids from the Antarctic sponge *Kirkpatrickia variolosa*. part 2: variolin A and N(3′)-methyl tetrahydrovariolin B. *Tetrahedron* **1994**, *50*, 3993–4000. [[CrossRef](#)]
4. Perry, N.B.; Ettouati, L.; Litaudon, M.; Blunt, J.W.; Munro, M.H.G.; Parkin, S.; Hope, H. Alkaloids from the Antarctic sponge *Kirkpatrickia variolosa*. *Tetrahedron* **1994**, *50*, 3987–3992. [[CrossRef](#)]
5. Diyabalanage, T.; Amsler, C.D.; McClintock, J.B.; Baker, B.J. Palmerolide a, a cytotoxic macrolide from the antarctic tunicate *Synoicum adareanum*. *J. Am. Chem. Soc.* **2006**, *128*, 5630–5631. [[CrossRef](#)] [[PubMed](#)]
6. von Salm, J.L.; Witowski, C.G.; Fleeman, R.M.; McClintock, J.B.; Amsler, C.D.; Shaw, L.N.; Baker, B.J. Darwinolide, a new diterpene scaffold that inhibits methicillin-resistant *Staphylococcus aureus* biofilm from the Antarctic sponge *Dendrilla membranosa*. *Org. Lett.* **2016**, *18*, 2596–2599. [[CrossRef](#)] [[PubMed](#)]

7. Thomas, S.A.L.; von Salm, J.L.; Clark, S.; Ferlita, S.; Nemani, P.; Azhari, A.; Rice, C.A.; Wilson, N.G.; Kyle, D.E.; Baker, B.J. Keikipukalides, furanocembrane diterpenes from the Antarctic deep sea octocoral *Plumerella delicatissima*. *J. Nat. Prod.* **2018**, *81*, 117–123. [[CrossRef](#)]
8. Shilling, A.J.; von Salm, J.L.; Sanchez, A.R.; Kee, Y.; Amsler, C.D.; McClintock, J.B.; Baker, B.J. Anverenes B-E, new polyhalogenated monoterpenes from the Antarctic red alga *Plocamium cartilagineum*. *Mar. Drugs* **2019**, *17*, 230. [[CrossRef](#)]
9. Knestrick, M.A.; Wilson, N.G.; Roth, A.; Adams, J.H.; Baker, B.J. Friomaramide, a highly modified linear hexapeptide from an Antarctic sponge *Inflatella coelosphaeroides*. *J. Nat. Prod.* **2019**, *82*, 2354–2358. [[CrossRef](#)]
10. Putra, M.Y.; Wibowo, J.T.; Murniasih, T. A review of chemistry and biological activities of the Indonesian octocorallia. *J. Appl. Pharm. Sci.* **2017**, *7*, 219–227.
11. Su, Y.D.; Su, J.H.; Hwang, T.L.; Wen, Z.H.; Sheu, J.H.; Wu, Y.C.; Sung, P.J. Briarane diterpenoids isolated from octocorals between 2014 and 2016. *Mar. Drugs* **2017**, *15*, 44. [[CrossRef](#)] [[PubMed](#)]
12. Liaw, C.C.; Shen, Y.C.; Lin, Y.S.; Hwang, T.L.; Kuo, Y.H.; Khalil, A.T. Frajunolides E-K, briarane diterpenes from *Junceella fragilis*. *J. Nat. Prod.* **2008**, *71*, 1551–1556. [[CrossRef](#)] [[PubMed](#)]
13. Chen, N.F.; Di Su, Y.; Hwang, T.L.; Liao, Z.J.; Tsui, K.H.; Wen, Z.H.; Wu, Y.C.; Sung, P.J.; Schmidt, T.J. Briarenols C-E, new polyoxygenated briaranes from the octocoral *Briareum excavatum*. *Molecules* **2017**, *22*, 475. [[CrossRef](#)] [[PubMed](#)]
14. Lei, H. Diterpenoids of gorgonian corals: chemistry and bioactivity. *Chem. Biodivers.* **2016**, *13*, 345–365. [[CrossRef](#)] [[PubMed](#)]
15. Li, C.; La, M.P.; Tang, H.; Sun, P.; Liu, B.S.; Zhuang, C.L.; Yi, Y.H.; Zhang, W. Chemistry and bioactivity of briaranes from the South China Sea gorgonian *Dichotella gemmacea*. *Mar. Drugs* **2016**, *14*, 201. [[CrossRef](#)] [[PubMed](#)]
16. Li, C.; La, M.-P.; Li, L.; Li, X.-B.; Tang, H.; Liu, B.-S.; Krohn, K.; Sun, P.; Yi, Y.-H.; Zhang, W. Bioactive 11,20-epoxy-3,5(16)-diene briarane diterpenoids from the South China Sea gorgonian *Dichotella gemmacea*. *J. Nat. Prod.* **2011**, *74*, 1658–1662. [[CrossRef](#)] [[PubMed](#)]
17. Pham, N.B.; Butler, M.S.; Healy, P.C.; Quinn, R.J. Anthoptilides A-E, new briarane diterpenes from the Australian sea pen *Anthoptilum cf. kukenthali*. **2000**, 318–321.
18. Garcia-Fernández, J. The genesis and evolution of homeobox gene clusters. *Nat. Rev. Genet.* **2005**, *6*, 881–892. [[CrossRef](#)]
19. Stern, M.; Gierse, A.; Tan, S.; Bicker, G. Human ntera2 cells as a predictive *in vitro* test system for developmental neurotoxicity. *Arch. Toxicol.* **2014**, *88*, 127–136. [[CrossRef](#)]
20. Tharmarajah, L.; Samarakoon, S.R.; Ediriweera, M.K.; Piyathilaka, P.; Tennekoon, K.H.; Senathilake, K.S.; Rajagopalan, U.; Galhena, P.B.; Thabrew, I. In vitro anticancer effect of gedunin on human teratocarcinoma (Ntera-2) cancer stem-like cells. *Biomed Res. Int.* **2017**, 2413197. [[CrossRef](#)]
21. France, S.C.; Hoover, L.L. Analysis of variation in mitochondrial DNA sequences (ND3, ND4L, MSH) among Octocorallia (= Alcyonaria)(Cnidaria: Anthozoa). *Bull. Biol. Soc. Wash.* **2001**, *10*, 110–118.
22. France, S.C.; Hoover, L.L. DNA sequences of the mitochondrial COI gene have low levels of divergence among deep-sea octocorals (Cnidaria: Anthozoa). *Hydrobiologia* **2002**, *471*, 149–155. [[CrossRef](#)]
23. Trifinopoulos, J.; Nguyen, L.T.; von Haeseler, A.; Minh, B.Q. W-IQ-TREE: A fast online phylogenetic tool for maximum likelihood analysis. *Nucl. Acids Res.* **2016**, *44*, W232–W235. [[CrossRef](#)] [[PubMed](#)]
24. Kalyanamoorthy, S.; Minh, B.; Wong, T.K.; Von Haeseler, A.; Jermin, L.S. ModelFinder: Fast model selection for accurate phylogenetic estimates. *Nature Methods* **2017**, *14*, 587–589. [[CrossRef](#)] [[PubMed](#)]
25. Hogan, R.I.; Hopkins, K.; Wheeler, A.J.; Allcock, A.L.; Yesson, C. Novel diversity in mitochondrial genomes of deep-sea Pennatulacea (Cnidaria: Anthozoa: Octocorallia). *Mitochondrial DNA Part A* **2019**, 1–14. [[CrossRef](#)] [[PubMed](#)]
26. Williams, G.C. The global diversity of sea pens (Cnidaria: Octocorallia: Pennatulacea). *PLoS one* **2011**, *6*, e22747. [[CrossRef](#)] [[PubMed](#)]
27. Bruker. *APEX3 User Manual*; Bruker AXS Inc.: Madison, WI, USA, 2016.
28. Bruker. *SAINTE v8.35a. Data Reduction Software*; Bruker AXS Inc.: Madison, WI, USA, 2017.
29. Sheldrick, G.M. SADABS program for empirical absorption correction. Ph.D. Thesis, University of Göttingen, Göttingen, Germany, 1996.
30. Sheldrick, G.M. SHELXT—Integrated space-group and crystal-structure determination. *Acta Crystallogr. Sect. A* **2015**, *A71*, 3–8. [[CrossRef](#)] [[PubMed](#)]

31. Sheldrick, G.M. Phase annealing in shelx-90: direct methods for larger structures. *Acta Crystallogr. Sect. A* **1990**, *46*, 467–473. [[CrossRef](#)]
32. Sheldrick, G.M. A short history of shelx. *Acta Crystallogr. Sect. A* **2008**, *64*, 112–122. [[CrossRef](#)] [[PubMed](#)]
33. Sheldrick, G.M. Crystal structure refinement with shelxl. *Acta Crystallogr. Sect. C* **2015**, *C71*, 3–8.
34. Dolomanov, O.V.; Bourhis, L.J.; Gildea, R.J.; Howard, J.A.K.; Puschmann, H. OLEX2: A complete structure solution, refinement and analysis program. *J. Appl. Crystallogr.* **2009**, *42*, 339–341. [[CrossRef](#)]
35. Spek, A.L. Structure validation in chemical crystallography. *Acta Crystallogr. Sect. D Biol. Crystallogr.* **2009**, *65*, 148–155. [[CrossRef](#)] [[PubMed](#)]
36. Hooft, R.W.W.; Straver, L.H.; Spek, A.L. Determination of absolute structure using Bayesian statistics on Bijvoet differences. *J. Appl. Crystallogr.* **2008**, *41*, 96–103. [[CrossRef](#)] [[PubMed](#)]



© 2019 by the authors. Licensee MDPI, Basel, Switzerland. This article is an open access article distributed under the terms and conditions of the Creative Commons Attribution (CC BY) license (<http://creativecommons.org/licenses/by/4.0/>).